Hindawi
Journal of Nanomaterials
Volume 2019, Article ID 6026390, 11 pages
https://doi.org/10.1155/2019/6026390

Research Article

Synthesis, Characterization, and Evaluation of Disulfide-Containing Polyethylenimine Derivative Functionalized Magnetic Carbon Nanotubes as an Efficient Gene Vector

Qiao Zhang, Fangzheng Yu, Ming Lei, Huili Fu, Guoping Yan, and Liang Li

School of Materials Science and Engineering, Wuhan Institute of Technology, Wuhan 430205, China

Correspondence should be addressed to Huili Fu; hlfuwit@163.com

Received 26 November 2018; Revised 11 January 2019; Accepted 22 January 2019; Published 27 March 2019

Academic Editor: Ruibing Wang

Magnetic nanoparticles have been widely developed as vectors in targeting drug and gene delivery. Disulfide-containing polyethylenimine derivative- (SSPEI-) functionalized magnetic carbon nanotubes (CNTs/Fe_3O_4-SSPEI) were synthesized as gene vector. Fourier transform infrared, transmission electron microscopy, X-ray diffraction, X-ray photoelectron spectroscopy, and thermogravimetric analysis were used to characterize CNTs/Fe_3O_4-SSPEI nanoparticles. The magnetic nanoparticles displayed typical superparamagnetic behavior and excellent dispersibility in water. Plasmid DNA could be bound by CNTs/Fe_3O_4-SSPEI to form the complexes. The sizes of complexes are about 400 nm, and the zeta potentials are positive at the w/w ratio over 6. CNTs/Fe_3O_4-SSPEI nanoparticles displayed higher transfection activity than did PEI (25 kDa), whereas the cytotoxicity was rather lower. Moreover, the transfection efficiency was further increased with the assistance of an external magnetic field. These results indicate that CNTs/Fe_3O_4-SSPEI nanoparticles would be a promising vector in targeted gene delivery.

1. Introduction

As a promising therapeutic method, gene therapy has shown considerable potential in genetic disorders, hereditary diseases, and some incurable diseases such as cancer [1, 2]. One obstacle in the application of gene therapy is the lack of efficient and safe gene transfer vectors. Viral vectors are regarded as having high transfection efficiency but are limited by their immunogenicity and safety. Nonviral vectors are nonimmunogenetic and easy to manufacture, which have attracted much attention and gotten more and more successes in in vitro and vivo applications [3–5]. Carbon nanotubes (CNTs) are a one-dimensional material with excellent physical and chemical properties, which have been used in many fields [6, 7]. Recently, carbon nanotubes (CNTs) have been developed as efficient gene vectors because of their larger surface area, which could conjugate DNA and siRNA via covalent and noncovalent interactions [8, 9].

Because of high hydrophobicity and poor biocompatibility, CNTs usually were demanded to be functionalized with hydrophilic molecules to achieve improved dispersion and biological properties [10]. In addition, although small interfering RNA (siRNA) and single-stranded DNA can be bound very strongly to pristine CNTs by interaction of π-stacking from CNTs and aromatic nucleotide bases from DNA, it is necessary to modify CNTs to bind double-stranded DNA or other types of large-sized nucleic acids [11]. The modification of CNTs as DNA vectors has been widely studied. The most classic approach is to incorporate some polycations such as polyethyleneimine (PEI) [12–14], polyamidoamine (PAMAM) [15, 16], and chitosan [17]. The cationic polymer-functionalized CNTs have improved dispersion and combining ability with DNA by the electrical reaction with negatively charged phosphate. The transfection efficiencies of functionalized CNTs are higher than that of cationic polymer alone.

Among those polycations, PEI is the most popular one, which was used to modify CNTs as gene vectors due to their high transfection activity. Nevertheless, the PEI-functionalized CNTs always display high cytotoxicity, which is mainly due to the introduction of PEI moiety [18]. As we know, high-molecular-weight polyethyleneimine with high

positive charge density leads to high transfection efficiency but also high cytotoxicity. On the contrary, the cytotoxicity of low-molecular-weight PEI is negligible, but the transfection activity is poor [19]. Therefore, some PEI derivatives with a biodegradable bonds have been synthesized, which can condense DNA efficiently during delivery to obtain high transfection efficiency and degrade after transfection to decrease the cytotoxicity [20, 21]. For example, cystamine bisacrylamide was used as a crosslinking agent to crosslink PEI (800 Da). The product is a PEI derivative containing a reversible disulfide bond, which exhibited higher transfection activity and lower cell toxicity [22].

Compared with virus vectors, lack of selectivity towards specific target cells is one of the key factors affecting the transfection efficiency of nonvirus vectors. In order to overcome this problem, lots of improvement methods have been studied [23, 24]. Among them, introducing a magnetic property to nonvirus gene vectors is an effective and convenient approach [25–27]. Through applying an applied magnetic field, the magnetic vectors can deliver more DNA to specific organs, tissues, or even cells. The increased amount of DNA that reached the target cells resulted in more chances of gene expression. Fe_3O_4 is the most traditional magnetic nanoparticle, which has been applied widely in the biomedical field in virtue of its superparamagnetism, biocompatibility, and biodegradability [28, 29]. However, naked Fe_3O_4 nanoparticles are easy to aggregate owing to the interaction between dipoles and their large surface area. To resolve this problem, Fe_3O_4 nanoparticles were always made with various coatings to inhibit aggregation [30]. In addition, Fe_3O_4 nanoparticles could be dispersed in CNTs to improve their stability, and the magnetic CNTs have been used in drug and gene delivery successfully [31].

In this study, Fe_3O_4-decorated magnetic CNTs were fabricated by a coprecipitation method. The disulfide-containing PEI (SSPEI) was synthesized through crosslinking the PEI with a molecular weight of 1.8 kDa by cystamine bisacrylamide. Then, magnetic CNTs were functionalized through grafting of SSPEI to the surface of the tubes to obtain CNTs/Fe_3O_4-SSPEI. The SSPEI on the surface of magnetic CNTs could provide the ability to bind DNA. In addition, DNA delivery efficiencies of magnetic CNTs could be further improved due to the increased amount of DNA to target cells by the attraction of a magnetic field. The SSPEI-functionalized magnetic CNTs were characterized using Fourier transform infrared spectroscopy, X-ray diffraction, transmission electron microscopy, X-ray photoelectron spectroscopy, and thermogravimetric analysis. The cytotoxicity and DNA-binding ability were also assayed. Then, the SSPEI-functionalized magnetic CNTs were employed as a gene vector to deliver two reporter plasmid DNAs to COS-7 and Hela cells to investigate the transfection efficiency.

2. Materials and Methods

2.1. Materials. Carboxyl functionalized multiwalled carbon nanotubes (CNTs-COOH) with purity of 98 (wt%), containing 1.23 wt% carboxyl groups, having an outer diameter of 20-30 nm and length of 0.5-2 μm were obtained from Chinese Academy of Sciences, Chengdu Organic Chemicals Co. Ltd. BPEI with the average molecular weight of 1.8 kDa and 25 kDa were obtained from Sigma-Aldrich. Thionyl chloride, triethylamine, acryloyl chloride, sodium hydroxide, 1-ethyl-3-(3-dimethylaminopropyl)carbodiimide hydrochloride (EDC), and N-hydroxysuccinimide (NHS) were purchased from Aladdin Co. (Shanghai, China). Acrylic acid, cyclohexane, triethylamine, dimethyl sulfoxide (DMSO), ammonium hydroxide, sodium bicarbonate, ferrous chloride tetrahydrate, ferric chloride hexahydrate, and hydroquinone were purchased from Shanghai Chemical Reagent Company and were used as received. Dulbecco's modified Eagle's medium (DMEM) was purchased from Gibco. Fetal bovine serum (FBS) was purchased from HyClone. Penicillin-streptomycin was purchased from Invitrogen. The Luciferase Assay System was purchased from Promega.

Hela and COS-7 cells were incubated in DMEM containing 10% FBS at 37°C and humidified air/5% CO_2. Cell cytotoxicity was assayed by using 3-[4,5-dimethylthiazol-2-yl]-2,5-diphenyltetrazoliumbromide (MTT) (Invitrogen). The DNA plasmids of pEGFP-C1 and pGL3-Luc were purchased from GENEWIZ (Suzhou, China), which were used as reporter gene.

2.2. Preparation of Magnetic CNTs. The magnetic CNTs/Fe_3O_4 nanocomposites were fabricated through the coprecipitation method. Briefly, 0.4 g carboxyl CNTs was added in 40 mL deionized water and sonicated at 50°C for 60 min. Then, 0.184 g $FeCl_3{\cdot}6H_2O$ and 0.068 g $FeCl_2{\cdot}4H_2O$ were added to a carboxyl CNT solution under N_2 protection and 10 mL ammonium hydroxide (8 M) was added dropwise. After reaction at 50°C for 30 min, the black precipitation was filtered and the deionized water was used to wash it to the pH of 7. Then, the product was dried for 24 h in an oven at 80°C.

2.3. Synthesis of Disulfide-Containing Polyethylenimine Derivative. Cystamine bisacrylamide (CBA) was synthesized according to our previous study [32]. First, 0.56 g cystamine dihydrochloride was dissolved with 25 mL deionized water. The solution was cooled to 0-5°C in an ice bath. Acryloyl chloride (0.1 mol) and NaOH (4 g) were dissolved in dichloromethane and deionized water, respectively, then both solutions were added simultaneously. After a continuous reaction for 16 h at room temperature, the obtained turbid solution was filtrated and washed five times with deionized water. Finally, the product was obtained by crystallization using acetate and dried for 24 h under vacuum at 40°C.

In order to obtain reducible SSPEI, 1.8 g of branched PEI 1.8 kDa and 0.684 g of CBA were dissolved with 20 mL and 10 L methanol, respectively. Then, the CBA solution was added to the PEI solution dropwise. The mixture solution was reacted for 48 h at 45°C under the protection of nitrogen. The solution was then acidified to pH 4 and diluted to 40 mL with water. Subsequently, the solution was dialyzed using dialysis membranes with molecular weight cutoffs of 3500 for 3 days. Finally, the product was obtained by lyophilizing for 2 days.

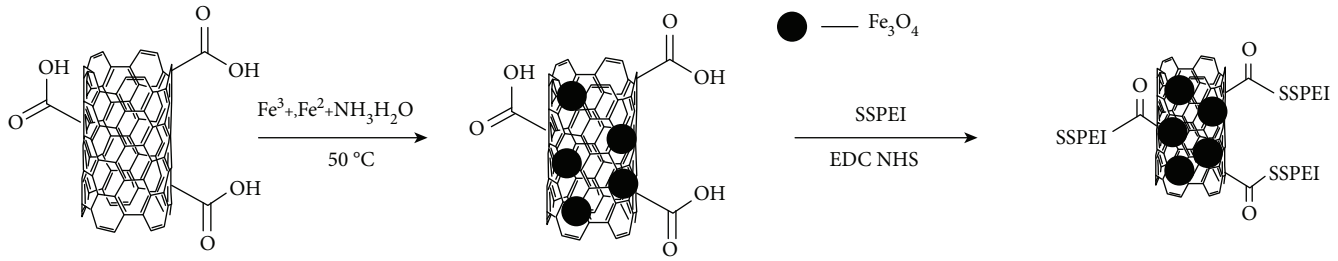

Scheme 1: Schematic illustration of the synthesis of CNTs/Fe_3O_4-SSPEI.

2.4. Synthesis of CNTs/Fe_3O_4-SSPEI. CNTs/Fe_3O_4 (200 mg) was suspended in 20 mL deionized water and ultrasonically dispersed at 50°C for 30 min. Then, EDC (105 mg) and NHS (82.4 mg) were added to activate the carboxyl groups of CNTs/Fe_3O_4. SSPEI (200 mg) was dissolved in 2 mL deionized water to prepare the SSPEI solution. Subsequently, the SSPEI solution was added and stirred for 24 h. After the reaction, the product was centrifuged at 20,000 × g for 20 min, then dispersed in deionized water again and dialyzed (MWCO:12000) for 48 h to remove the unreacted SSPEI and activating agent. Lastly, CNTs/Fe_3O_4-SSPEI in a black powdered form was obtained after lyophilization for 48 h.

2.5. Characterization. The Fourier transform infrared (FT-IR) spectra of CNTs/Fe_3O_4-SSPEI was recorded on Nicolet Impact 420 in the range of 400-4000 cm^{-1}. The morphology of CNTs/Fe_3O_4-SSPEI was conducted by JEM-2100F field emission electron microscopy (TEM, JEOL, Japan). X-ray diffraction (XRD) analysis was performed using an X-ray diffractometer (D/Max-IIIc, Japan) using Cu-Kα radiation ($\lambda = 1.5406$ Å) at room temperature. The elemental compositions of CNTs/Fe_3O_4-SSPEI were investigated by X-ray photoelectron spectroscopy (XPS, Thermo Fisher, 250XI). Thermogravimetric analyzer (TGA) measurement of CNTs/Fe_3O_4-SSPEI was performed by a TGA STA 409 PC under nitrogen in the temperature from 30 to 800°C with an increasing rate of 5°C min^{-1}. The magnetic properties were measured using a vibrating specimen magnetometer (SQUID VSM) to the field strength of 2 T.

2.6. Preparation of Vector/DNA Complexes. To prepare CNT/Fe_3O_4-SSPEI and DNA complexes, 50 μL DNA solution (containing 1 μg pEGFP-C1 or pGL3-Luc) and 50 μL CNTs/Fe_3O_4-SSPEI solution were mixed at various w/w ratios of CNTs/Fe_3O_4-SSPEI to DNA, then vortexed and incubated for 30 min.

The PEI/DNA complexes at the N/P ratio of 10 were prepared as follows: 50 μL DNA solution (containing 1 μg pEGFP-C1 or pGL3-Luc) and 50 μL PEI of Mw 25 kDa or 1.8 kDa solution (containing 1.33 μg PEI) were mixed. Then, the mixture was vortexed and incubated for 30 min.

2.7. Size and Zeta Potential Measurements. 1 mL CNT/Fe_3O_4-SSPEI/DNA complex solution containing 5 μg pGL3-Luc was used to measure the mean size and surface charge. The assay was performed by a Zetasizer Nano ZS (Malvern, ZEN 3600, UK). The mean ± standard deviation (SD) was given according to three independent measurements.

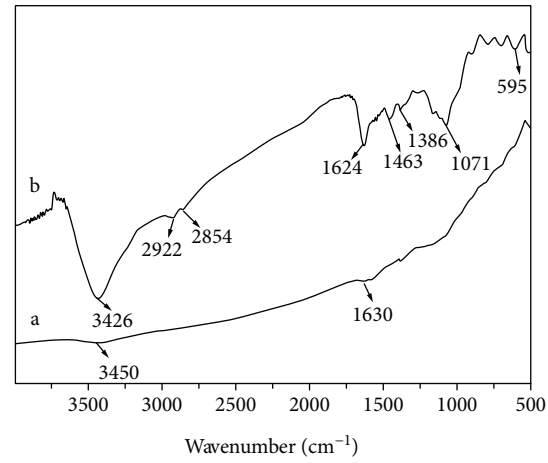

Figure 1: FTIR spectra of carboxyl CNTs (a) and CNTs/Fe_3O_4-SSPEI (b).

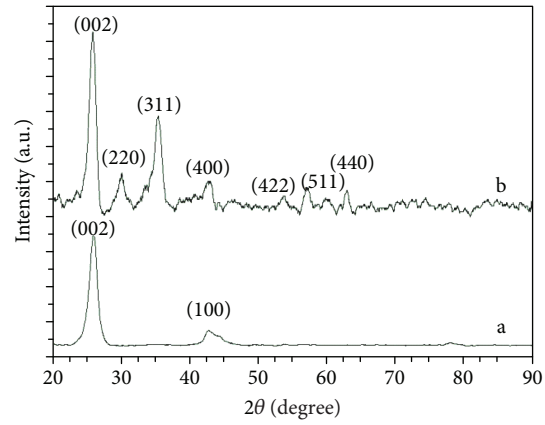

Figure 2: X-ray diffractograms of carboxyl CNTs (a) and CNTs/Fe_3O_4-SSPEI (b).

2.8. In Vitro Cytotoxicity. The cytotoxicity of CNTs/Fe_3O_4-SSPEI and PEI (Mw 25 kDa) was examined with COS-7 cells using MTT assay. 6×10^3 cells were seeded in each well of 96-well plates and incubated for 24 h. Then, the medium

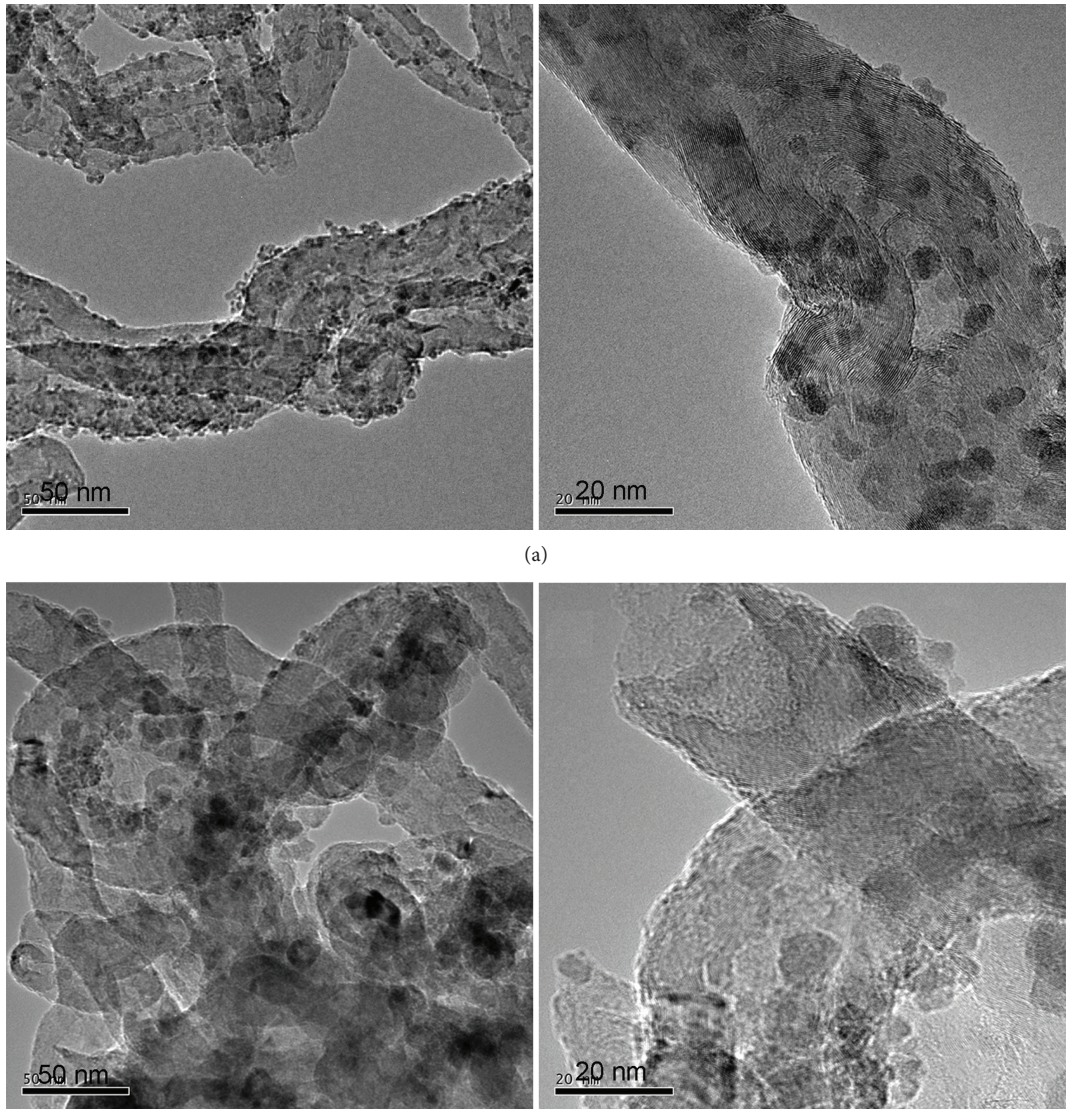

Figure 3: TEM images of CNTs/Fe_3O_4 (a) and CNTs/Fe_3O_4-SSPEI (b).

was discarded and the fresh medium as well as certain CNTs/Fe_3O_4-SSPEI or PEI were added. The medium was removed again after 48 h. A fresh medium and 20 μL of MTT (5 mg/mL) solution were added and then incubated for 4 h. The medium was taken out, and 150 μL DMSO was added. The relative cell viability was analyzed at absorbance wavelengths of 570 nm by a microplate reader (Molecular Devices SpectraMax i3x).

2.9. In Vitro Transfections. COS-7 and Hela cells were transfected with CNT/Fe_3O_4-SSPEI/DNA complexes to evaluate the transfection efficiency. Cells were seeded in a 24-well plate with 1 mL DMEM containing 10% FBS. The density is 6×10^4 cells per well. 1 mL serum-free DMEM was used to replace the medium after 24 h. Then, 100 μL complex-containing solution was added into each well. For the group of the transfection in an applied magnetic field, a magnet (0.2 T, M+) was placed under the plate. After incubation for 4 h, the medium was removed and a fresh medium was added. Then, the cells were further incubated for 44 h. The transfection occurred without the magnetic field (M-) as a contrast.

For the expression of luciferase, plasmid pGL-3 was used in transfection of COS-7 and Hela cells. The cells were lysed using 200 μL reporter lysis buffer after gene transfection. The luciferase activity was measured by a luminometer (Lumat LB 9507, Berthold) according to the procedure of the Luciferase Assay System (Promega). The total protein was determined by BCA protein assay kit (Pierce). The transfection efficiency was expressed by luciferase activity in RLU per mg protein.

For the expression of green fluorescent proteins, plasmid pEGFP-C1 was used in transfection of COS-7 cells. The weight ratio of CNTs/Fe_3O_4-SSPEI/DNA is 8. The PEI/DNA complexes prepared by 1.8 kDa and 25 kDa PEI were used as control. The micrographs of green fluorescent light spots were recorded by an inverted microscope installed with Image-Pro Plus software under magnification of 200.

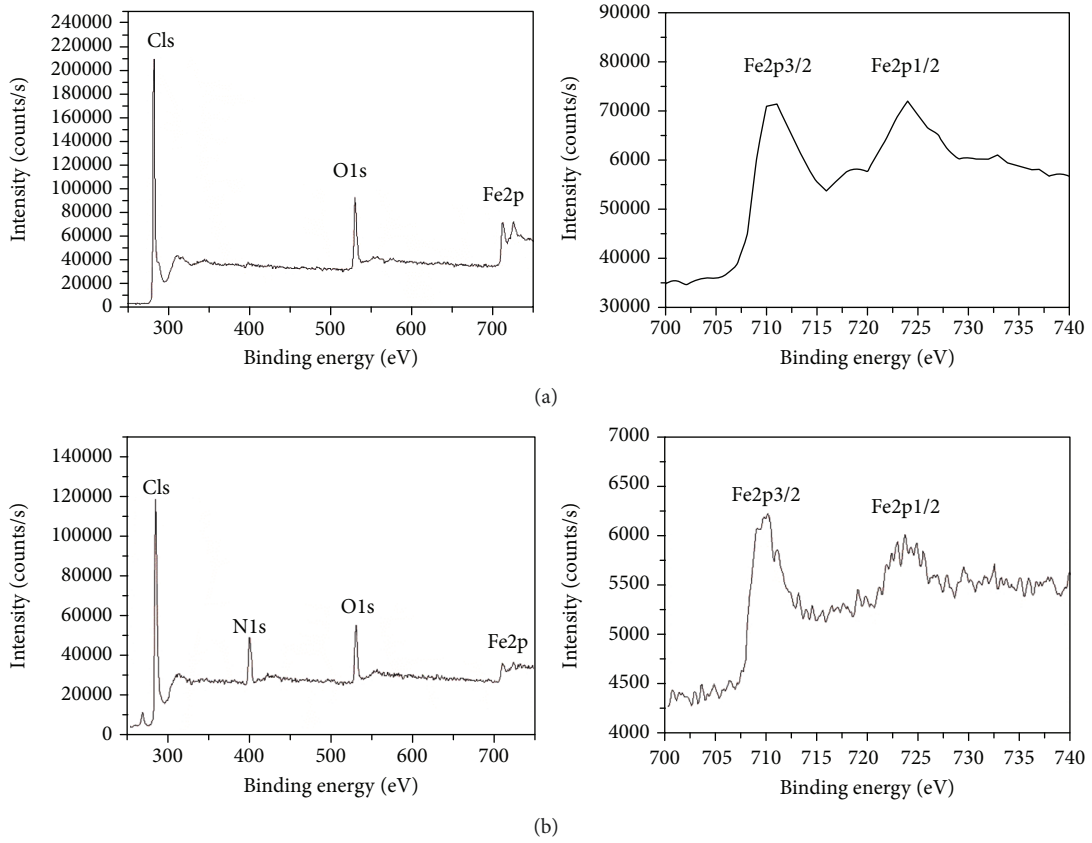

Figure 4: XPS spectrum of CNTs/Fe_3O_4 (a) and CNTs/Fe_3O_4-SSPEI (b).

2.10. In Vitro Cellular Uptake of Vector/DNA Complexes. Plasmid of pGL-3 was labeled by YOYO-1. The vector/DNA complexes at the w/w ratio of 8 were prepared according to the preceding method. 3.0×10^5 COS-7 cells were seeded in a culture dish with 2 mL medium; the serum-free DMEM was used to replace the medium after 24 h. Then, the vector/DNA complex solution was added to the medium and incubated for 4 h at 37°C with or without a magnetic field. The cells were washed several times with PBS, and the nuclei were strained with Hoechst 33258 for 15 min at 37°C. Then, the cells were also washed several times with PBS. At last, the cells were observed by confocal laser scanning microscopy (CLSM Nikon Ni-E C2+) at the magnification of 400x.

2.11. Statistical Analysis. The statistical differences between two sets of data were performed by Student's t-test. Results were considered significant difference if $P < 0.05$ (*).

3. Results and Discussion

3.1. The Preparation and Characterization of CNTs/Fe_3O_4-SSPEI. CNTs have shown great potential applications as drug and gene vectors owing to their unique mechanical, physical, and chemical properties. Fe_3O_4 nanoparticles are the most traditional magnetic materials with outstanding superparamagnetism and biocompatibility. It was reported that CNTs and Fe_3O_4 can form magnetic nanoparticles through coprecipitation [31]. In order to bind double-stranded DNA effectively, CNTs have to be functionalized with a positive charge. In this study, a disulfide-containing PEI derivative was synthesized by cross-linking low-molecular-weight branched 1.8 kDa PEI with cystamine bisacrylamide. The average molecular weight (Mn) was 11.0 kDa, and the polydispersity (Mw/Mn) was 1.23. Then, the magnetic CNT was functionalized with a disulfide-containing PEI derivative to obtain a magnetic gene vector. Disulfide-containing PEI can be degraded by intracellular glutathione to reduce the cytotoxicity and release DNA. The synthesis route is illustrated in Scheme 1.

FTIR spectroscopy was employed to characterize the formation of CNTs/Fe_3O_4-SSPEI. As shown in Figure 1 (curve a), the peaks of 3450 cm^{-1} and 1630 cm^{-1} are the -OH stretch and -C=O stretch from carboxyl groups of carboxyl CNTs, respectively. In Figure 1(b), the broad and strong peak at 3426 cm^{-1} is associated to -NH stretching vibrations of SSPEI and the -OH group in CNTs [33]. The peaks of 1624, 1463, and 1386 cm^{-1} are the characteristic bands of -CO-NH- stretching, which indicated that the SSPEI molecules were successfully introduced on CNTs/Fe_3O_4 [16]. The bands around 600 cm^{-1} are the characteristic of iron oxides [34]. In addition, the peaks at 2922 cm^{-1} and 2854 cm^{-1} as well as the peak at 1071 cm^{-1} are assigned to the C-H stretching vibrations and C-O-C stretching vibration, respectively [35].

The chemical composition and crystal phases of CNTs/Fe_3O_4-SSPEI nanocomposites were determined by X-ray powder diffraction. Figure 2 shows the XRD patterns

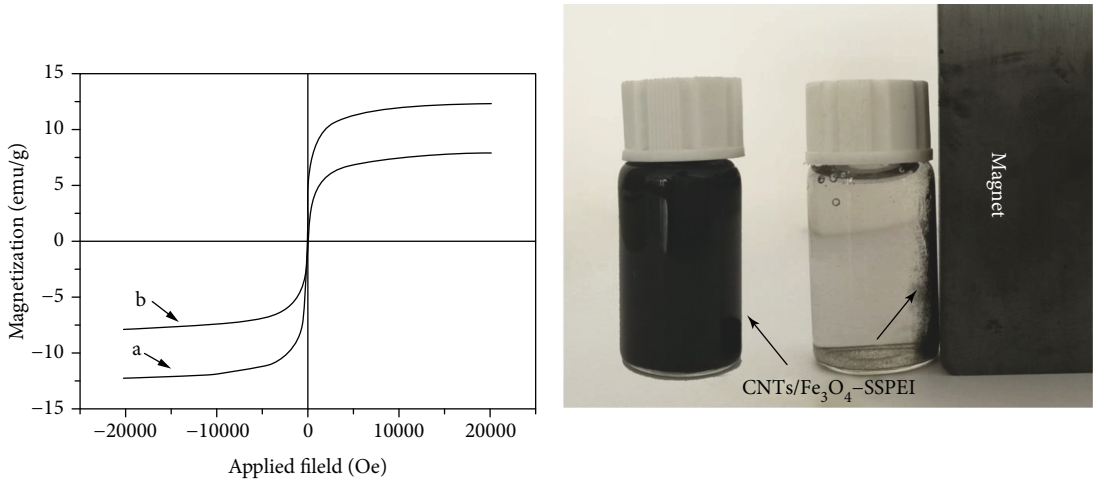

Figure 5: Magnetic properties of samples. (a) Magnetization curves of $CNTs/Fe_3O_4$ (a) and $CNTs/Fe_3O_4$-SSPEI (b); (b) photograph of magnetic $CNTs/Fe_3O_4$-SSPEI nanoparticles dispersed in water and its response to a magnet.

of carboxyl CNTs and $CNTs/Fe_3O_4$-SSPEI nanocomposites. The diffraction peaks at 26.0° and 42.7° (Figure 2(a)) are assigned to the (0 0 2) and (1 0 0) reflection planes of carboxyl CNTs, respectively. The diffraction peaks in Figure 2(b) demonstrate that the magnetic nanoparticles in $CNTs/Fe_3O_4$-SSPEI are Fe_3O_4 crystal. This is because six planes of (2 2 0), (3 1 1), (4 0 0), (4 2 2), (5 1 1), and (4 4 0) were detected, which are the characteristic planes of the standard Fe_3O_4 crystal with a spinel structure [34].

The morphology and distribution of Fe_3O_4 nanoparticles in carboxyl CNTs were explored by TEM. As shown in Figure 3(a), Fe_3O_4 nanoparticles are attached to the inner and surface of CNTs and dispersed uniformly. The average size is about 8-10 nm. As we know, because of high surface energy, Fe_3O_4 nanoparticles are easy to aggregate. Some polymer coatings were used to stabilize Fe_3O_4 nanoparticles. However, the Fe_3O_4 nanoparticles were dispersed in CNTs homogeneously without any coating, and the size is very small. This is because of the strong interaction between the Fe_3O_4 nanoparticles and CNTs, which prevented the aggregation of Fe_3O_4 nanoparticles. A similar phenomenon was also reported in a previous study [36]. Figure 3(b) illustrates the morphology of $CNTs/Fe_3O_4$-SSPEI, which is similar to that of $CNTs/Fe_3O_4$. However, Fe_3O_4 nanoparticles became blurred due to the SSPEI coating on the surface of $CNTs/Fe_3O_4$.

The elemental compositions of $CNTs/Fe_3O_4$ and $CNTs/Fe_3O_4$-SSPEI were investigated using XPS. As shown in Figure 4(a), the bends at 284, 530, and 711 eV are related to the energetic distribution of C 1s, O 1s, and Fe 2p orbits, respectively. The bends at 711 and 724.9 eV were also detected, which are attributed to Fe 2p1/2 and Fe 2p3/2 from Fe chemical states in Fe_3O_4 [35].This result also confirms that the magnetic component in magnetic carbon nanotubes is Fe_3O_4. The molar contents of carbon, oxygen, and iron are 84.2%, 4.28%, and 11.51%, respectively. Compared with $CNTs/Fe_3O_4$, the XPS spectrum of $CNTs/Fe3O4\text{-}SSPEI_3O_4$-SSPEI shows an additional component at a binding energy of 398.29 eV assigned to N 1s

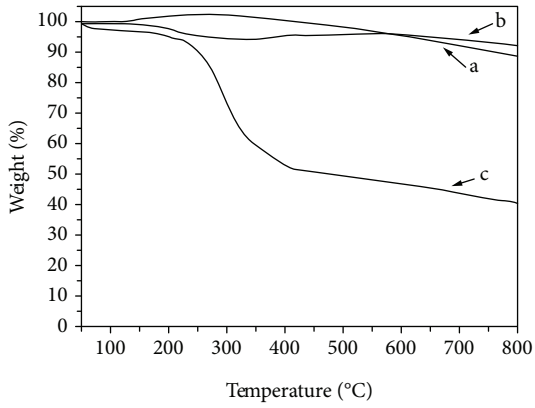

Figure 6: TGA profiles of carboxyl CNTs (A), $CNTs/Fe_3O_4$ (B), and $CNTs/Fe_3O_4$-SSPEI (C).

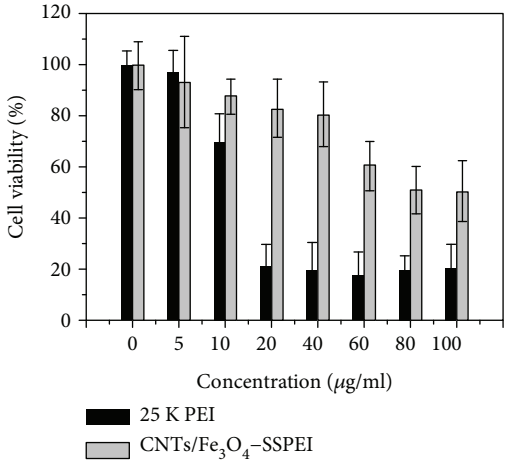

Figure 7: Cytotoxicity induced by $CNTs/Fe_3O_4$-SSPEI and PEI (25 kDa) in COS-7 cells. Data are shown as mean ± SD ($n = 5$).

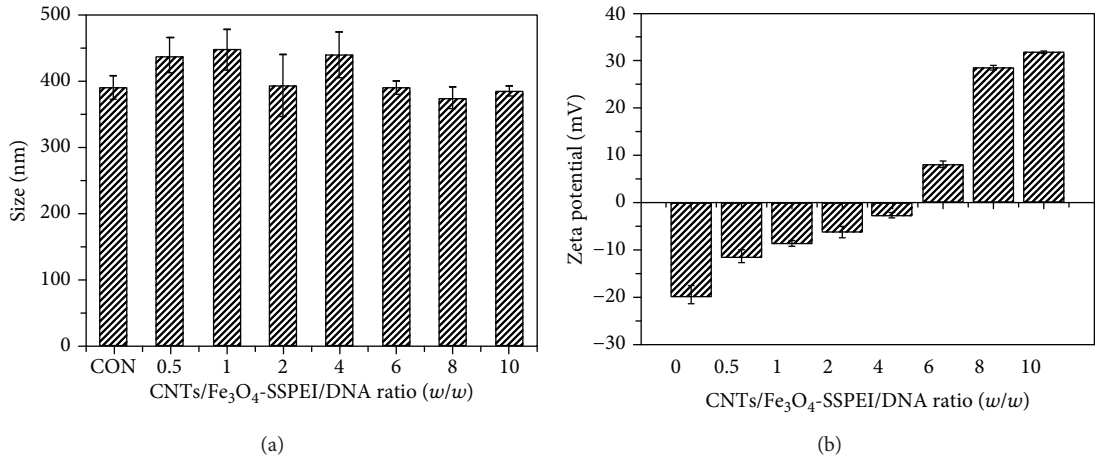

(a) (b)

Figure 8: The particle sizes (a) and zeta potential (b) of CNTs/Fe_3O_4-SSPEI/DNA particles with different mass ratios of CNTs/Fe_3O_4-SSPEI/DNA. The size of CNTs/Fe_3O_4-SSPEI nanoparticles was measured as control (CON). Data are shown as mean ± SD ($n = 3$).

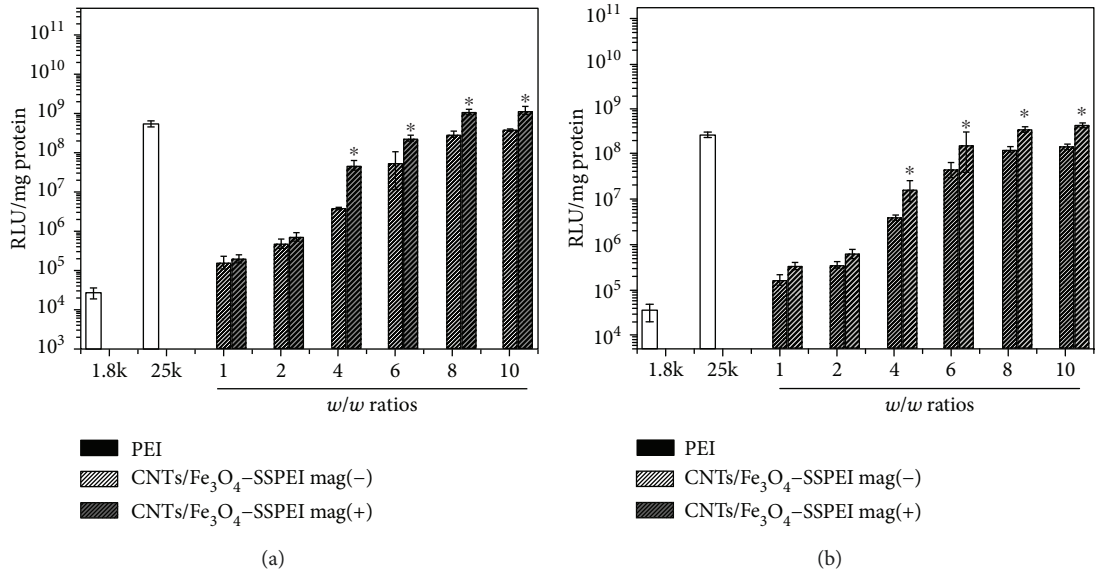

(a) (b)

Figure 9: The transfection efficiency of CNTs/Fe_3O_4-SSPEI/DNA complexes in COS-7 cells (a) and Hela cells (b). Data are shown as mean ± SD ($n = 3$). (*$P < 0.05$ as compared with the data at the same w/w ratios without an external magnetic field).

orbital. The presence of a nitrogen atom in the CNTs/Fe_3O_4-SSPEI spectrum confirms successful grafting of SSPEI on the surface of the CNT/Fe_3O_4 composite. The molar contents of carbon, oxygen, nitrogen, and iron are 77.39%, 9.24%, 11.79%, and 1.59%, respectively.

The magnetic properties of CNTs/Fe_3O_4 and CNTs/Fe_3O_4-SSPEI were tested using VSM with a maximal applied field of 20 kOe. The result is shown in Figure 5(a). Both samples display a typical superparamagnetic behavior. The saturation magnetization of CNTs/Fe_3O_4 and CNTs/Fe_3O_4-SSPEI are 12.3 and 7.9 emu·g^{-1}, respectively. Both are much lower than that of bulk Fe_3O_4, which is about 60 emu·g^{-1}. There are two reasons for the decreased saturation magnetization value of CNTs/Fe_3O_4. One is the decreased weight content of Fe_3O_4 moiety in the composite. The other is contributed to the small size of Fe_3O_4 [30, 37]. Due to the functionalization with SSPEI, the saturation magnetization of CNTs/Fe_3O_4-SSPEI further decreased. Although the magnetic property is reduced compared to bulk Fe_3O_4, CNTs/Fe_3O_4-SSPEI displayed sufficient magnetization to an external magnet. As shown in Figure 5(b), the CNTs/Fe_3O_4-SSPEI nanoparticles disperse stably in water and can be attracted well to a magnet.

3.2. Thermogravimetric Analysis. TGA was further used to measure the content of SSPEI moiety grafted onto the surface of magnetic CNTs. As we know, both CNTs and Fe_3O_4 nanoparticles have good thermal stability. Therefore, a very small weight loss was recorded in Figure 6 (curves A and B) up to 800°C. On the other hand, the SSPEI-functionalized CNT sample (curve C) shows a sharp weight decrease from 200°C to 400°C. This is mainly due to the thermal

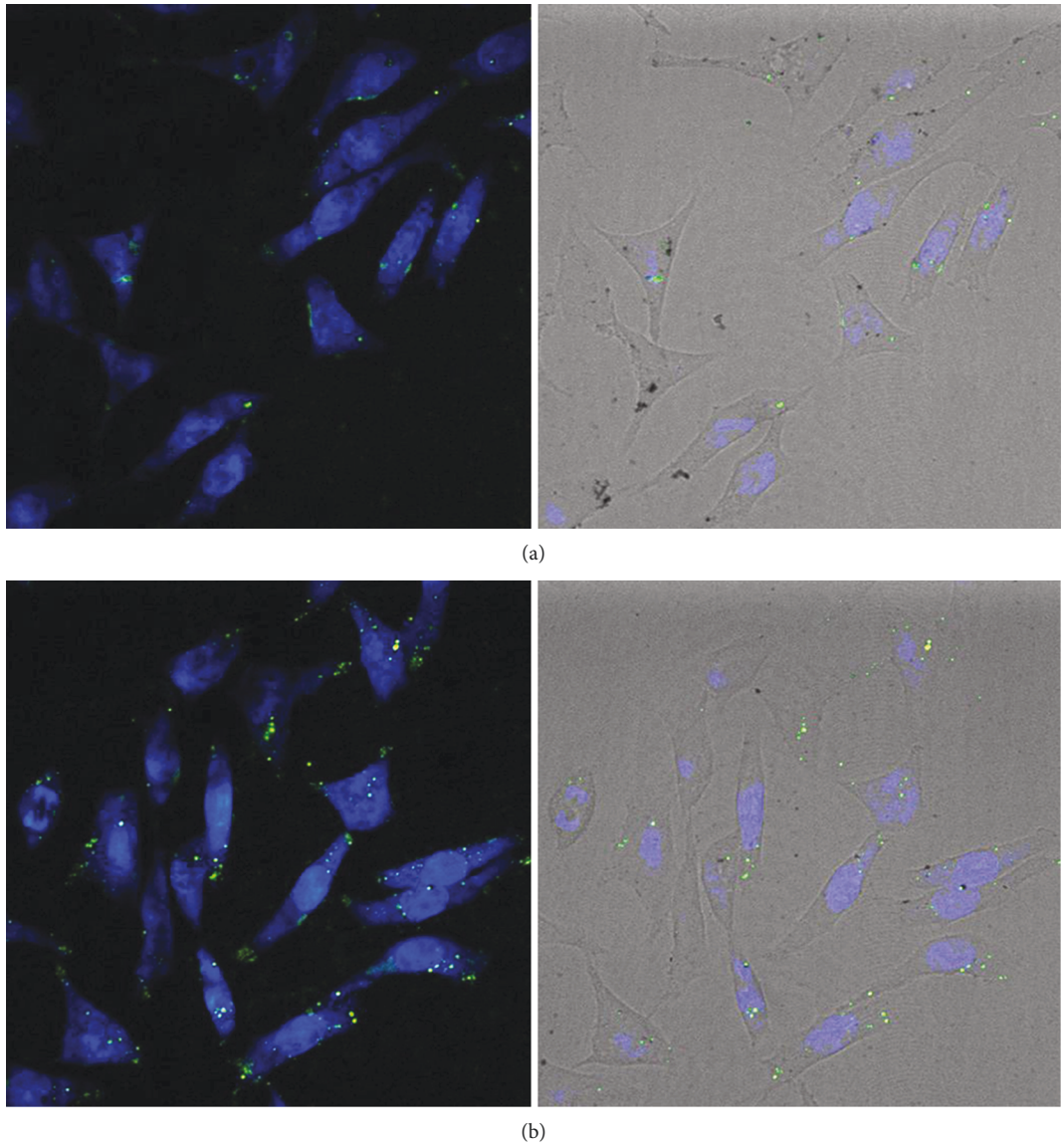

(a)

(b)

Figure 10: Confocal images of COS-7 cells after incubation with CNTs/Fe_3O_4-SSPEI/DNA complexes without an external magnetic field (a) and with an external magnetic field (b). The weight ratio of CNTs/Fe_3O_4-SSPEI/DNA is 8.

decomposition of SSPEI. The mass content of SSPEI in CNTs/Fe_3O_4-SSPEI estimated by TGA is about 40%.

3.3. In Vitro Cytotoxicity. We tested the cytotoxicity of CNTs/Fe_3O_4-SSPEI by MTT assay in COS-7 cells. As shown in Figure 7, cell viability decreased slightly with an increase in the concentration of CNTs/Fe_3O_4-SSPEI. However, it still presented high cell viability (>80%) at the concentration of 40 μg/mL. On the contrary, the cell viability of 25 kDa PEI decreased drastically to 20% at the same concentration. This result indicated that CNTs/Fe_3O_4-SSPEI displayed remarkably lower cytotoxicity than 25 kDa PEI did. As we know, carbon nanotubes have nonignorable cytotoxicity, which can be reduced by functionalization of specific polymers. Despite that the PEI-modified carbon nanotubes have lower cytotoxicity than pristine carbon nanotubes [18], PEI itself has high cytotoxicity due to nondegradability and high positive charge density. In the previous report, because of the presence of reversible disulfide bonds, SSPEI has low cytotoxicity, which can be degraded to small-molecular-weight PEI with low cytotoxicity [22]. Therefore, SSPEI was used to modify the magnetic carbon nanotubes.

3.4. Particle Size and Zeta Potential. For nonviral gene vectors with high transfection activity, the ability to bind DNA to form particles of suitable size and positive charge is essential. As shown in Figure 8(a), the particle sizes of CNTs/Fe_3O_4-SSPEI was measured as control, which is 390 nm. The particle sizes of CNTs/Fe_3O_4-SSPEI/DNA at various ratios are around 400 nm. Plasmid DNAs are flexible rolling-circle, which are attached to the surface of CNTs/Fe_3O_4-SSPEI nanoparticles like a coating via electrostatic interaction. The thickness is only a few nanometers. Therefore, the particle sizes do not significantly increase

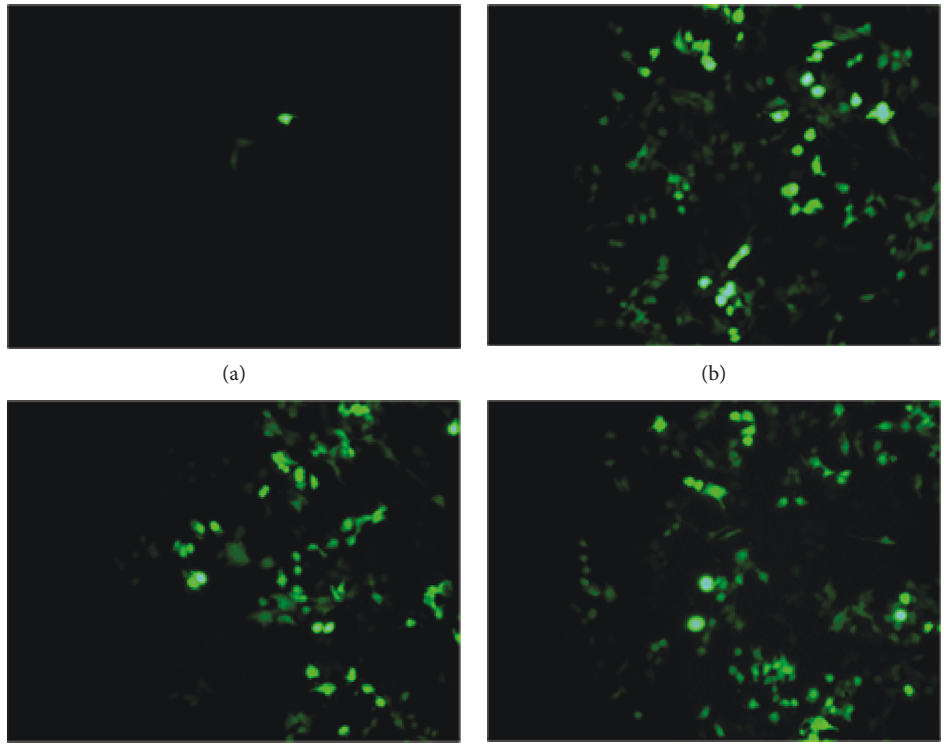

Figure 11: Enhanced green fluorescent protein expression in COS-7 cells transfected with 1.8 kDa PEI/DNA (a) and 25 kDa PEI/DNA (b) at N/P of 10, as well as CNTs/Fe_3O_4-SSPEI/DNA complexes at a weight ratio of 8 without an external magnetic field (c) and with an external magnetic field (d).

after binding with plasmid DNAs. The zeta potential of CNTs/Fe_3O_4-SSPEI/DNA complexes increased with the increase in *w*/*w* ratios (Figure 8(b)). The value changed from negative to positive when the weight ratio of CNTs/Fe_3O_4-SSPEI and DNA is over 6. The positively charged complexes as a result of excess CNTs/Fe_3O_4-SSPEI would favor the cellular uptake as well as endosomal escape.

3.5. In Vitro Transfection. The transfection efficiencies of CNTs/Fe_3O_4-SSPEI/DNA complexes at the weight ratio ranging from 1 to 10 were evaluated in COS-7 and Hela cells (Figure 9). Optimized 25 kDa PEI/DNA and 1.8 kDa PEI/DNA complexes were used as the control. As shown in Figure 9(a), the luciferase expressions in COS-7 cells transfected with CNTs/Fe_3O_4-SSPEI/DNA complexes increased significantly with the increase in *w*/*w* ratios. At the same *w*/*w* ratio, CNTs/Fe_3O_4-SSPEI exhibited a much higher gene transfection activity than 1.8 kDa PEI did. The optimal luciferase expression efficiency was achieved at the *w*/*w* ratio of 8. It is well known that the high positive surface charge of nanoparticles facilitates to bind the negatively charged cell membranes and thus to be taken up via endocytosis [38]. At the *w*/*w* ratio of 8, the zeta potential of the CNTs/Fe_3O_4-SSPEI/DNA complex is +28.7 mV, which is the critical factor for high transfection efficiency. In addition, when placing a magnet under the cell plate during transfection, the transfection activity of CNTs/Fe_3O_4-SSPEI was significantly enhanced than that without the magnet at the same *w*/*w* ratio ($P < 0.05$). For example, at the *w*/*w* ratio of 6, the transfection efficiency increased 4-fold under an applied magnetic field of 0.2 T. The reason for this result was attributed to the increased sedimentation rates of CNTs/Fe_3O_4-SSPEI/DNA complexes on the cell surface under the applied magnetic field. In order to further confirm this mechanism, we used confocal laser scanning microscopy to observe the cell uptake in the presence of a magnetic field. As shown in Figure 10, with the assistance of a magnetic field, more green fluorescence dots were observed in cells, which confirmed that the external magnetic field could increase the cellular uptake. As in previous studies, the cellular endocytosis of magnetic nanoparticles can be enhanced in the presence of an external magnetic field [37, 39]. Our result is in accordance with the literatures. More CNTs/Fe_3O_4-SSPEI/DNA complexes were internalized by cells with the assistance of a magnetic field, which resulted in increased transfection efficiency.

Optimized transfection efficiency mediated by CNTs/Fe_3O_4-SSPEI/DNA complexes under the magnetic field was higher than that by 25 kDa PEI/DNA complexes. The reasons for the high transfection ability might be attributed to the combinational factors including low cytotoxicity, suitable particle size, and an accelerated sedimentation rate under an external magnetic field. The trends of luciferase expressions are similar in Hela cells (Figure 9(b)). The transfection efficiency of CNTs/Fe_3O_4-SSPEI/DNA complexes could be markedly increased in

the influence of a magnetic field at the corresponding w/w ratio.

Another reporter gene pEGFP-C1 was used to further confirm the transfection efficiency of CNTs/Fe_3O_4-SSPEI in COS-7 cells. The images of gene transfection are shown in Figure 11. Being consistent with the result of the luciferase experiment, the images also indicated that the green fluorescent protein expressions of CNTs/Fe_3O_4-SSPEI/DNA complex-treated cells were enhanced under the external magnetic field. There are more green fluorescent spots in COS-7 cells transfected by CNTs/Fe_3O_4-SSPEI nanoparticles with the assistance of a magnetic field than that without a magnetic field.

4. Conclusions

In this study, magnetic CNTs (CNTs/Fe_3O_4) were prepared through a conventional coprecipitation method, then magnetic CNTs were further functionalized with disulfide-containing PEI (SSPEI) as a gene vector. The FTIR, XRD, XPS, TEM, and TGA studies demonstrated the chemical composition and structure of CNTs/Fe_3O_4-SSPEI. CNTs/Fe_3O_4-SSPEI had good dispersibility and stability in water and were strongly attractive to an external magnet. The particle size and zeta potential measurements of CNTs/Fe_3O_4-SSPEI/DNA showed that CNTs/Fe_3O_4-SSPEI were able to bind DNA efficiently. More importantly, CNTs/Fe_3O_4-SSPEI nanoparticles displayed a higher transfection activity and lower cytotoxicity compared with PEI 25 k. Furthermore, the transfection efficiency could be further increased with the assistance of an applied magnetic field. These results indicate that CNTs/Fe_3O_4-SSPEI nanoparticles would be a promising targeted gene vector in gene therapy.

Data Availability

The data used to support the findings of this study have been deposited in the Figshare repository doi:10.6084/m9.figshare.7405748.

Conflicts of Interest

The authors declare that there is no conflict of interests.

Acknowledgments

This work was supported by the National Natural Science Foundation of China [Grant No. 51503165]; National Key Research and Development Program [Grant No. 2018YFB1105502], and Science Foundation of Wuhan Institute of Technology [Grant No. K201808].

References

[1] D. E. Dorer and D. M. Nettelbeck, "Targeting cancer by transcriptional control in cancer gene therapy and viral oncolysis," *Advanced Drug Delivery Reviews*, vol. 61, no. 7-8, pp. 554–571, 2009.

[2] C. Booth, H. B. Gaspar, and A. J. Thrasher, "Treating immunodeficiency through HSC gene therapy," *Trends in Molecular Medicine*, vol. 22, no. 4, pp. 317–327, 2016.

[3] M. A. Mintzer and E. E. Simanek, "Nonviral vectors for gene delivery," *Chemical Reviews*, vol. 109, no. 2, pp. 259–302, 2009.

[4] M. Karimi, A. Ghasemi, P. Sahandi Zangabad et al., "Smart micro/nanoparticles in stimulus-responsive drug/gene delivery systems," *Chemical Society Reviews*, vol. 45, no. 5, pp. 1457–1501, 2016.

[5] L. Jin, X. Zeng, M. Liu, Y. Deng, and N. He, "Current progress in gene delivery technology based on chemical methods and nano-carriers," *Theranostics*, vol. 4, no. 3, pp. 240–255, 2014.

[6] S. Iijima, "Helical microtubules of graphitic carbon," *Nature*, vol. 354, no. 6348, pp. 56–58, 1991.

[7] S. Dong, J. Zhou, D. Hui et al., "Interaction between edge dislocations and amorphous interphase in carbon nanotubes reinforced metal matrix nanocomposites incorporating interface effect," *International Journal of Solids and Structures*, vol. 51, no. 5, pp. 1149–1163, 2014.

[8] R. Alshehri, A. M. Ilyas, A. Hasan, A. Arnaout, F. Ahmed, and A. Memic, "Carbon nanotubes in biomedical applications: factors, mechanisms, and remedies of toxicity: miniperspective," *Journal of Medicinal Chemistry*, vol. 59, no. 18, pp. 8149–8167, 2016.

[9] K. Bates and K. Kostarelos, "Carbon nanotubes as vectors for gene therapy: past achievements, present challenges and future goals," *Advanced Drug Delivery Reviews*, vol. 65, no. 15, pp. 2023–2033, 2013.

[10] N. K. Mehra, V. Mishra, and N. K. Jain, "A review of ligand tethered surface engineered carbon nanotubes," *Biomaterials*, vol. 35, no. 4, pp. 1267–1283, 2014.

[11] G. Bartholomeusz, P. Cherukuri, J. Kingston et al., "In vivo therapeutic silencing of hypoxia-inducible factor 1 alpha (HIF-1α) using single-walled carbon nanotubes noncovalently coated with siRNA," *Nano Research*, vol. 2, no. 4, pp. 279–291, 2009.

[12] Y. P. Huang, I. J. Lin, C. C. Chen, Y. C. Hsu, C. C. Chang, and M. J. Lee, "Delivery of small interfering RNAs in human cervical cancer cells by polyethylenimine-functionalized carbon nanotubes," *Nanoscale Research Letters*, vol. 8, no. 1, p. 267, 2013.

[13] A. H. Nia, A. Amini, S. Taghavi, H. Eshghi, K. Abnous, and M. Ramezani, "A facile Friedel-Crafts acylation for the synthesis of polyethylenimine-grafted multi-walled carbon nanotubes as efficient gene delivery vectors," *International Journal of Pharmaceutics*, vol. 502, no. 1-2, pp. 125–137, 2016.

[14] D. Pantarotto, R. Singh, D. McCarthy et al., "Functionalized carbon nanotubes for plasmid DNA gene delivery," *Angewandte Chemie*, vol. 43, no. 39, pp. 5242–5246, 2004.

[15] M. Liu, B. Chen, Y. Xue et al., "Polyamidoamine-grafted multi-walled carbon nanotubes for gene delivery: synthesis, transfection and intracellular trafficking," *Bioconjugate Chemistry*, vol. 22, no. 11, pp. 2237–2243, 2011.

[16] B. Pan, D. Cui, P. Xu et al., "Synthesis and characterization of polyamidoamine dendrimer-coated multi-walled carbon nanotubes and their application in gene delivery systems," *Nanotechnology*, vol. 20, no. 12, pp. 125101–125187, 2009.

[17] X. Liu, Y. Zhang, D. Ma et al., "Biocompatible multi-walled carbon nanotube-chitosan-folic acid nanoparticle hybrids as GFP gene delivery materials," *Colloids and Surfaces B Biointerfaces*, vol. 111, no. 11, pp. 224–231, 2013.

[18] B. Z. Yu, J. F. Ma, and W. X. Li, "Polyethylenimine-modified multiwalled carbon nanotubes for plasmid DNA gene delivery," *Nature Precedings*, vol. 1, no. 1, pp. 2753–2757, 2009.

[19] S. M. Moghimi, P. Symonds, J. C. Murray, A. C. Hunter, G. Debska, and A. Szewczyk, "A two-stage poly(ethylenimine)-mediated cytotoxicity: implications for gene transfer/therapy," *Molecular Therapy*, vol. 11, no. 6, pp. 990–995, 2005.

[20] M. P. Xiong, M. Laird Forrest, G. Ton, A. Zhao, N. M. Davies, and G. S. Kwon, "Poly(aspartate-g-PEI800), a polyethylenimine analogue of low toxicity and high transfection efficiency for gene delivery," *Biomaterials*, vol. 28, no. 32, pp. 4889–4900, 2007.

[21] S. Taranejoo, J. Liu, P. Verma, and K. J. Hourigan, "A review of the developments of characteristics of PEI derivatives for gene delivery applications," *Journal of Applied Polymer Science*, vol. 132, no. 25, p. 42096, 2015.

[22] Y. X. Sun, X. Zeng, Q. F. Meng, X. Z. Zhang, S. X. Cheng, and R. X. Zhuo, "The influence of RGD addition on the gene transfer characteristics of disulfide-containing polyethyleneimine/DNA complexes," *Biomaterials*, vol. 29, no. 32, pp. 4356–4365, 2009.

[23] J. Yao, Y. Fan, Y. Li, and L. Huang, "Strategies on the nuclear-targeted delivery of genes," *Journal of Drug Targeting*, vol. 21, no. 10, pp. 926–939, 2013.

[24] S. Ghiamkazemi, A. Amanzadeh, R. Dinarvand, M. Rafiee-Tehrani, and M. Amini, "Synthesis, and characterization, and evaluation of cellular effects of the FOL-PEG-g-PEI-GAL nanoparticles as a potential non-viral vector for gene delivery," *Journal of Nanomaterials*, vol. 2010, Article ID 863136, 10 pages, 2010.

[25] K. Ulbrich, K. Holá, V. Šubr, A. Bakandritsos, J. Tuček, and R. Zbořil, "Targeted drug delivery with polymers and magnetic nanoparticles: covalent and noncovalent approaches, release control, and clinical studies," *Chemical Reviews*, vol. 116, no. 9, pp. 5338–5431, 2016.

[26] I. Belyanina, O. Kolovskaya, S. Zamay, A. Gargaun, T. Zamay, and A. Kichkailo, "Targeted magnetic nanotheranostics of cancer," *Molecules*, vol. 22, no. 6, pp. 975–993, 2017.

[27] J. Dobson, "Magnetic micro- and nano-particle-based targeting for drug and gene delivery," *Nanomedicine*, vol. 1, no. 1, pp. 31–37, 2006.

[28] L. Shen, B. Li, and Y. Qiao, "Fe_3O_4 nanoparticles in targeted drug/gene delivery systems," *Materials*, vol. 11, no. 2, pp. 324–353, 2018.

[29] L. Chen, Y. Xue, X. Xia et al., "A redox stimuli-responsive superparamagnetic nanogel with chemically anchored DOX for enhanced anticancer efficacy and low systemic adverse effects," *Journal of Materials Chemistry B*, vol. 3, no. 46, pp. 8949–8962, 2015.

[30] R. Liu, Y. Qiao, Y. Xu, X. Ma, and Z. Li, "A facile controlled in-situ synthesis of monodisperse magnetic carbon nanotubes nanocomposites using water-ethylene glycol mixed solvents," *Journal of Alloys and Compounds*, vol. 657, pp. 138–143, 2016.

[31] L. Wang, J. Shi, Y. Hao et al., "Magnetic multi-walled carbon nanotubes for tumor theranostics," *Journal of Biomedical Nanotechnology*, vol. 11, no. 9, pp. 1653–1661, 2015.

[32] Q. Zhang, M. Lei, S. Huang et al., "Preparation, characterization, and properties of disulfide-containing polyethyleneimine grafted carbon nanotubes," *Fullerenes, Nanotubes and Carbon Nanostructures*, vol. 25, no. 6, pp. 386–390, 2017.

[33] H. Moradian, H. Fasehee, H. Keshvari, and S. Faghihi, "Poly(ethyleneimine) functionalized carbon nanotubes as efficient nano-vector for transfecting mesenchymal stem cells," *Colloids and Surfaces B Biointerfaces*, vol. 122, no. 10, pp. 115–125, 2014.

[34] M. H. Moghim and S. M. Zebarjad, "Fabrication and structural characterization of multi-walled carbon nanotube/Fe_3O_4 nanocomposite," *Journal of Inorganic and Organometallic Polymers*, vol. 25, no. 5, pp. 1260–1266, 2015.

[35] E. G. Uc-Cayetano, F. Avilés, J. V. Cauich-Rodríguez et al., "Influence of nanotube physicochemical properties on the decoration of multiwall carbon nanotubes with magnetic particles," *Journal of Nanoparticle Research*, vol. 16, no. 1, p. 2192, 2014.

[36] N. D. Quyen Chau, C. Ménard-Moyon, K. Kostarelos, and A. Bianco, "Multifunctional carbon nanomaterial hybrids for magnetic manipulation and targeting," *Biochemical and Biophysical Research Communications*, vol. 468, no. 3, pp. 454–462, 2015.

[37] S. W. Zheng, G. Liu, R. Y. Hong, H. Z. Li, Y. G. Li, and D. G. Wei, "Preparation and characterization of magnetic gene vectors for targeting gene delivery," *Applied Surface Science*, vol. 259, no. 16, pp. 201–207, 2012.

[38] R. Kircheis, L. Wightman, and E. Wagner, "Design and gene delivery activity of modified polyethylenimines," *Advanced Drug Delivery Reviews*, vol. 53, no. 3, pp. 341–358, 2001.

[39] R. Namgung, K. Singha, M. K. Yu et al., "Hybrid superparamagnetic iron oxide nanoparticle-branched polyethylenimine magnetoplexes for gene transfection of vascular endothelial cells," *Biomaterials*, vol. 31, no. 14, pp. 4204–4213, 2010.